

Article

Not peer-reviewed version

Influence of pH Value on Microstructure and Properties of Strontium Phosphate Chemical Conversion Coatings on Titanium

[Guochao Gu](#) , [Yibo Li](#) , [Kangqing Zuo](#) , [Guiyong Xiao](#) *

Posted Date: 7 August 2023

doi: 10.20944/preprints202308.0578.v1

Keywords: Titanium; phosphate chemical conversion; coating; strontium phosphate



Preprints.org is a free multidiscipline platform providing preprint service that is dedicated to making early versions of research outputs permanently available and citable. Preprints posted at Preprints.org appear in Web of Science, Crossref, Google Scholar, Scilit, Europe PMC.

Copyright: This is an open access article distributed under the Creative Commons Attribution License which permits unrestricted use, distribution, and reproduction in any medium, provided the original work is properly cited.

Article

Influence of pH Value on Microstructure and Properties of Strontium Phosphate Chemical Conversion Coatings on Titanium

Guochao Gu ^{1,2}, Yibo Li ^{1,2}, Kangqing Zuo ^{1,2} and Guiyong Xiao ^{1,2,*}

¹ Key Laboratory for Liquid-solid Structural Evolution and Processing of Materials, Ministry of Education, Shandong University, Ji'nan 250061, People's Republic of China

² School of Materials Science and Engineering, Shandong University, Ji'nan 250061, People's Republic of China

* Correspondence: xiaoguiyong@sdu.edu.cn

Abstract: Strontium (Sr) is a trace element in human body that able to promote bone formation and inhibit bone absorption. The conversion coating of strontium phosphate (Sr-P) on the surface of titanium (Ti) can improve its biological properties, and has a wide application prospect in the fields of dentistry and orthopedics. In this present study, Sr-P coatings with SrHPO_4 and $\text{Sr}_3(\text{PO}_4)_2$ crystals on Ti are prepared by phosphate chemical conversion (PCC) treatment. And the effect of pH on the properties of Sr-P coatings is researched. The results prove that phase composition, morphology and corrosion resistance of coated Ti are different with the pH values in PCC solution. The morphologies of conversion deposition on Ti change from plat-like to cluster-like, and then homogeneous microcrystals, as pH value changed from 2.50 to 3.25. Only discrete SrHPO_4 crystals are generating on substrate at lower pH value, while relative stable $\text{Sr}_3(\text{PO}_4)_2$ and SrHPO_4 crystals are growing and subsequently forming an integrated coating on Ti as pH is higher than 2.50. The corrosion resistance of coated Ti improves comparing with that of bare Ti because of forming Sr-P coatings with $\text{Sr}_3(\text{PO}_4)_2$ phase. In addition, it is indicated that the Sr-P coatings can improve the adhesion and differentiation of BMSCs.

Keywords: titanium; phosphate chemical conversion; coating; strontium phosphate

1. Introduction

Titanium (Ti) and its alloys have been greatly interested in dentistry and orthopedics surgery owing to their suitable mechanical property, as well as good chemical resistance *in vivo* with the help of their oxide film [1]. However, the corrosion resistance of Ti implants will be greatly reduced with long-term interaction with body fluids. When it comes to the surgical application, the sustainability of Ti implant is questioned because of toxic ions releasing by corrosion in the harsh condition *in vivo*, involving chloride ion and proteins. What's more, it is hard for Ti to achieve chemical bonds with bone due to its essential bio-inertness[2]. Therefore, various surface modifications are applied to optimize the properties of Ti and its alloys [3, 4]. Chemical conversion treatment is regarded as the simple and effective ways to improve the surface properties of metals [5]. Because of its comparatively low-cost and environment-friendly characteristic, phosphate chemical conversion (PCC) treatment has been widely adopted to augment the corrosion resistance and bioactivity of metal implants [6, 7]. In the last decade, the PCC technology has been broadly used in the fields of the surface modification for biomedical metallic materials such as magnesium, titanium and zinc alloys [8-11]. In addition, some biofunctional cations, such as calcium (Ca^{2+}), magnesium (Mg^{2+}), zinc (Zn^{2+}), strontium ($\text{Sr}^{4+}/\text{Sr}^{2+}$) were also commonly used as PCC coated materials[12, 13].

Strontium (Sr^{2+}) is a bone-seeking trace element which is incorporated in bone in a similar way like Ca^{2+} . It accounts about 0.035% of mineral component in the skeleton system[14]. It is reported that proper amount of Sr^{2+} can efficiently stimulate bone formation and be applied partially to

enhance the mechanical properties of bone tissues, because it can replace a moderate amount of Ca^{2+} in the lattice, which leads to making the array of atoms more compact and reduction of lattice defects [15]. Moreover, literature was proved that Sr could improve corrosion resistance and stimulate bone formation by accelerating differentiation of preosteoblast and increasing the number of osteoblasts [16]. Meanwhile, Sr can restrain the activity of osteoclasts and then decrease the number of osteoclasts and inhibits bone resorption [17]. Based on the evidence supplied above, Sr has a promising prospect of application in clinical application. For strontium phosphates (Sr-P), SrHPO_4 and $\text{Sr}_3(\text{PO}_4)_2$ as main compounds have been taken attention recently. Especially, SrHPO_4 can be considered to be an ion exchanger biomaterial for holding both HPO_4^{2-} and Sr^{2+} ions [18]. $\text{Sr}_3(\text{PO}_4)_2$ also has been researched because it is a precursor of strontium apatite as a great biomaterials [19].

Previous research results indicated that parameters affecting the microstructure and properties of chemical conversion coatings include reaction temperature and time, as well as pH value of solution [20-22]. Among them, the pH value was one of the most effective factors in the formation of coating, which can affect the formation rate and the properties of coatings, such as coating mass, phase, morphology, on metallic substrates [21]. Literatures illustrated that the metal ions phosphate can be deposited easily on metal surface if the pH value of reaction mixture exceeds its solubility limit [23]. Hence, it is important to investigate the effect of pH value in PCC solution on the microstructure and properties of coatings on Ti substrates.

However, few reports have involved in fabrication of Sr-P coatings on Ti substrate, as well as the relationship between its properties and pH value in reaction solution by PCC treatment. Thus, the aim of this study is to explore the feasibility of phosphate chemical conversion coatings dopants with strontium and investigate the effect of pH values on the microstructure and properties, such as wettability, anticorrosion and cytocompatibility, of that coatings on Ti.

2. Materials and experimental methods

2.1. Surface pretreatment

Commercially Ti was processed into $\text{Ø}10\text{mm} \times 3\text{mm}$ cylinders as substrates. All the Ti samples were polished to obtain homogeneous roughness. Then, the substrates were degreased in 80 g/L sodium hydroxide (NaOH) solution at 50°C for 15min. Next, the cylinders were etched with 2% hydrofluoric acid (HF) at room temperature for 15s. Finally, the samples were immersed in 3.00 g/L colloidal titanium phosphate to increase the nucleation points on Ti surface. The bare Ti disks was used as control.

2.2. Phosphate chemical conversion

The PCC treatment was similar to that reported previously [24, 25]. Briefly, pretreated Ti specimens were put into PCC solution, that contained 0.20mol/L NaH_2PO_4 , 0.40mol/L $\text{Sr}(\text{NO}_3)_2$, 2.00g/L NaNO_2 and 5.00g/L Iron powder. After aging for 24h, pH value was adjusted to 2.50-3.25 using H_3PO_4 or NaOH. Finally, the pretreated Ti samples were incubated in the PCC solution for 30 min at 60°C .

2.3. Electrochemical measurements

Electrochemical impedance spectroscopy (EIS) of PCC coatings were carried out on an automatic laboratory corrosion measurement system (PARSTAT 2273). And a classical three-electrode cell was set up in the simulated body fluid (SBF), at a scan rate 2 mV/s^{-1} . The saturated calomel electrode (SCE), platinum, and the sample coupon with 1 cm^2 exposed area were used as reference, counter, and working electrodes in the three-electrode cell (CHI660E), respectively. The Tafel polarization curve was calculated using a constant voltage scan rate. And then, the equilibrium potential (E_{corr}), the corrosion current (I_{corr}) and the anode/cathode Tafel slope (β_a/β_c) was deduced. The polarization resistance (R_p) was calculated according to the following equation.

$$R_p = \frac{\beta_a \cdot |\beta_c|}{2.303 \cdot I_{corr} \cdot (\beta_a + |\beta_c|)}$$

2.4. Cell culture

BMSCs were cultured in fresh Dulbecco's modified Eagle's medium (DMEM, Gibco) containing 10% (v/v) fetal bovine serum (FBS, Gibco), 1% penicillin/streptomycin in a humidified atmosphere at 37°C and 5% CO₂. The polished Ti and its coatings were sterilized using ultraviolet for 1h. And then, BMSCs were seeded onto the samples in 24-well plates at a density of 2×10⁴ cell/well. The proliferation rates of BMSCs cells grown on different samples were assessed using a cell counting kit-8 (CCK-8 kit, Dojindo Molecular Technologies). The BMSCs cells with three replicates were seeded into a 24-well plate and pre-incubated for 48h to allow for complete adherence before conducting CCK-8 assay. All the CCK-8 values were normalized to the control, which represents 100% cell viability.

2.5. Characterization of samples

The morphologies of PCC samples and BMSCs on the coated Ti were tested using scanning electron microscope (FE-SEM, HATA-CHI SU-70) equipped with an energy dispersive spectrometer (EDS). All samples were sputtered by nano golden particles before testing. Phase composition of coatings was examined by an X-ray diffractometer (XRD, Rigaku D/max-γB) using a Cu-Kα radiation operated at 40 kV and 100 mA, with a scan rate of 4°/min and a scan step of 0.02° from 10° to 80°.

3. Results

3.1. Phase composition

The XRD patterns of PCC coatings obtained with different pH value at 60°C for 30 min are shown in Figure 1. The result of XRD patterns shows that effective conversion coating is not formed on Ti surface at pH is 2.50. While, SrHPO₄ and Sr₃(PO₄)₂ phases are detected on the surface of Ti, as pH exceeds 2.50. Specifically, when pH value is 2.75, SrHPO₄ crystals begin to form on the Ti substrate. In addition, some weak peaks of Sr₃(PO₄)₂ appear on the coating with pH=2.75. Meanwhile, the peaks of Ti become weaker, indicating that Ti sample is covered by conversion coating. As the pH value increases to 3.00, the relative intensity of the peaks of SrHPO₄ become stronger, which indicates an increase in covered area and coating thickness. Meanwhile, the peaks of Sr₃(PO₄)₂ obviously appear at pH 3.00. As pH up to 3.25, Figure 1 shows that strong diffraction peaks of Sr₃(PO₄)₂ are detected. The peaks at 25.50°, 27.08° and 31.36° are strong and sharp, implying the good crystallinity of SrHPO₄ and Sr₃(PO₄)₂ [26].

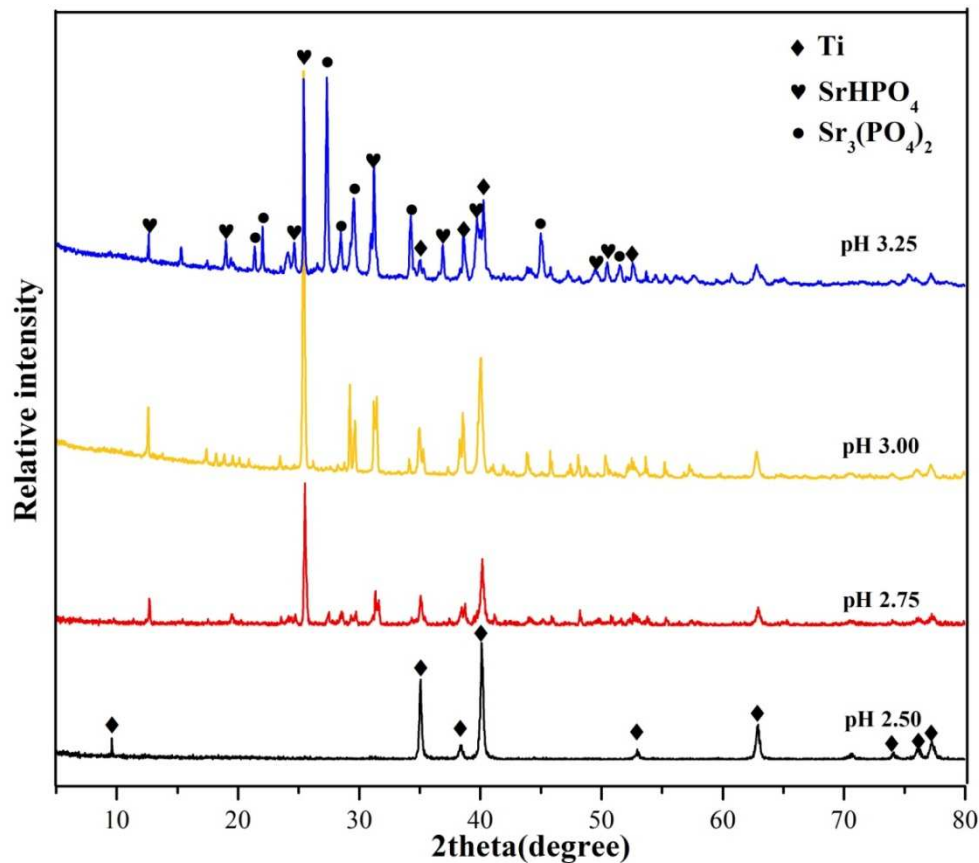


Figure 1. XRD patterns of conversion coatings on Ti with pH value from 2.50-3.25.

3.2. Microstructure

Figure 2 shows the surface morphology of conversion coatings on Ti fabricated by PCC treatments at various pH values. The results show that only a few sporadic plate-like conversion crystals are distributed on the Ti surface as pH is 2.50. And the conversion coatings are formed as pH exceeds 2.50. Generally speaking, as pH up to 2.75, almost all the area of Ti substrate is covered by plate-like and cluster-like crystals. And the morphology of conversion crystals on Ti becomes finer and denser when pH value increases to 3.25. Moreover, the cluster-like crystals are distributed between the plate-like crystals, as shown in Figure 2B. The high magnification images (Figure 2 B1-B2) indicate that some microcrystals exist in the long axis direction of plate-like crystal, which proved that the crystals will continuously grow along that way in subsequent steps. In addition, the cluster-like crystals are uncompleted, like numerous flakes being put together. As pH value increased to 3.00 (Figure 2C), almost all plate-like crystals disappear, and are replaced by cluster-like crystals. Different from the cluster-like crystals at pH 2.75, the cluster-like crystals at pH 3.00 are completed and compact. The high magnified images (Figure 2C1-C2) shows that the cluster-like coating consists of compact flaky crystals with a nucleation core. When pH is 3.25, as shown in Figure 2D, the Ti substrate is almost covered by dense and tiny plate-like crystals with directionless growth. These small crystals are not in clusters but distribute evenly on the Ti surface, as shown in Figure 2D1-D2.

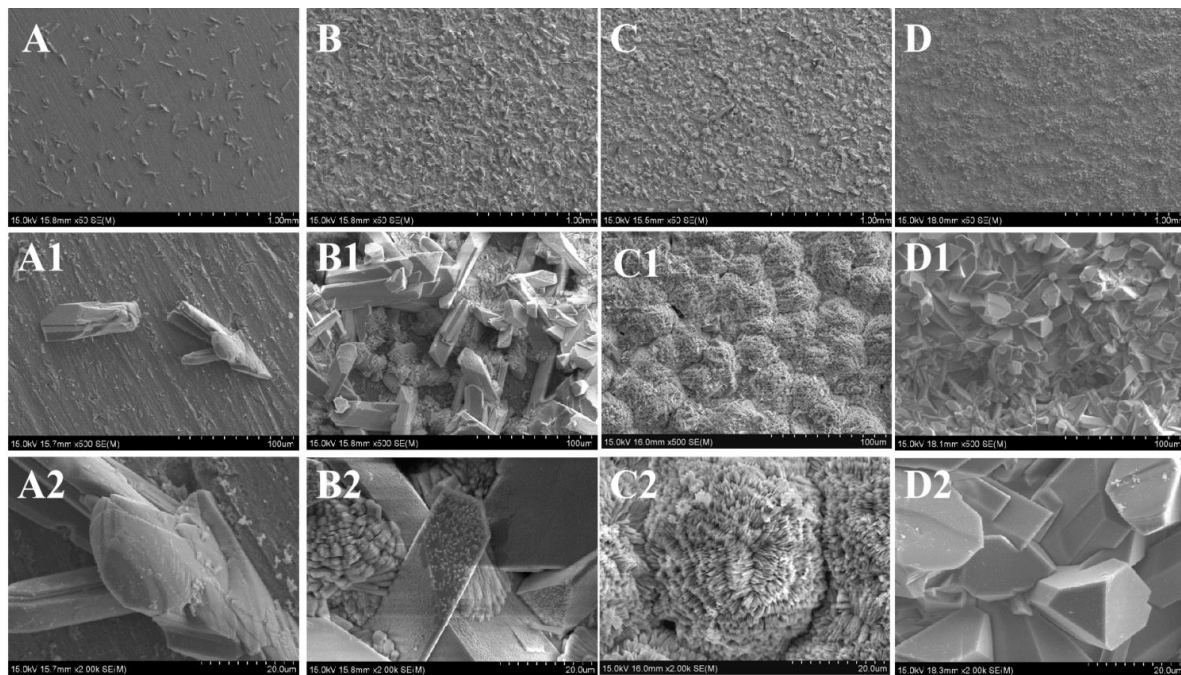


Figure 2. Surface morphology of conversion coatings by PCC treatment at various pH values. (A) 2.50, (B) 2.75, (C) 3.00, (D) 3.25.

Table 1 lists the compositions of conversion crystals detected by EDS analysis. Table 1 shows that the PCC coatings are mainly composed of C, P, Ti, Sr and O at pH value from 2.50 to 3.25. When pH is 2.50 and 2.75, it is seen that the quality of Sr and P is nearly equality, which suggests that crystals are the SrHPO_4 phase. At pH 3.00 and 3.25, the ratios of Sr/P in coating crystals are 1.12 and 1.25, while that ratios are 1.00 and 1.50 in SrHPO_4 and $\text{Sr}_3(\text{PO}_4)_2$ respectively. That indicates that the coating crystals formed at pH is 3.00 and 3.25 is the mixture of SrHPO_4 and $\text{Sr}_3(\text{PO}_4)_2$ phase.

Table 1. EDS analysis of conversion crystals by PCC treatment at various pH values.

pH value	O	P	Sr	Ti	C	Sr/P
2.50	67.59	9.56	10.10	2.81	9.94	1.06
2.75	62.13	13.52	13.85	----	10.50	1.02
3.00	70.17	14.02	15.68	0.13	----	1.12
3.25	57.52	13.20	16.52	----	12.76	1.25

Note: Data in this table means atom%.

3.3. Corrosion Characteristics.

Figure 3 presents the potentiodynamic polarization curves of bare Ti and PCC coated samples treated by different pH values in SBF. The parameters of electrochemical corrosion of different samples are listed in **Table 2**. Since there are only a few crystals on the surface of Ti at pH=2.50 and no coating is formed at all, its electrochemical data was not presented in this part. The result clearly illustrates that the open circuit potential (E_{corr}) value is a function of processing pH values. And E_{corr} of samples is improving, and corrosion current density (I_{corr}) is oppositely decreasing with increasing of pH value of PCC solution. In addition, the bare Ti has the lowest E_{corr} and higher I_{corr} , comparing with other coated Ti substrates. In addition, Table 2 shows that the R_p values of coated Ti are greater than that of bare sample. This proves that the SrHPO_4 phosphate coatings can prove the anti-corrosion properties comparing with bare Ti sample. Meanwhile, the coating with pH=3.00 has the highest R_p value and E_{corr} compared to other samples, which indicates that it has the best corrosion resistance. These results are closely related to the microstructure of the conversion coatings on Ti surface.

Table 2. Electrochemical corrosion parameters determined by potentiodynamic polarization curves of the bare Ti and coated samples with different pH values. Data are shown as mean \pm SD, n = 3.

Sample	E_{corr} (V)	I_{corr} ($\times 10^{-8}$ A/cm 2)	β_a (V \cdot dec $^{-1}$)	$-\beta_c$ (V \cdot dec $^{-1}$)	R_p ($\times 10^4$ $\Omega\cdot$ cm 2)
Bare Ti	-0.426 ± 0.006	12.67 ± 4.35	0.129 ± 0.007	0.107 ± 0.005	11.230 ± 0.675
pH=2.75	-0.212 ± 0.009	28.32 ± 6.24	0.221 ± 0.010	0.179 ± 0.019	15.163 ± 0.022
pH=3.00	-0.325 ± 0.011	30.04 ± 4.54	0.399 ± 0.006	0.088 ± 0.013	24.122 ± 0.286
pH=3.25	-0.072 ± 0.016	53.89 ± 3.46	0.445 ± 0.001	0.215 ± 0.002	16.026 ± 0.954

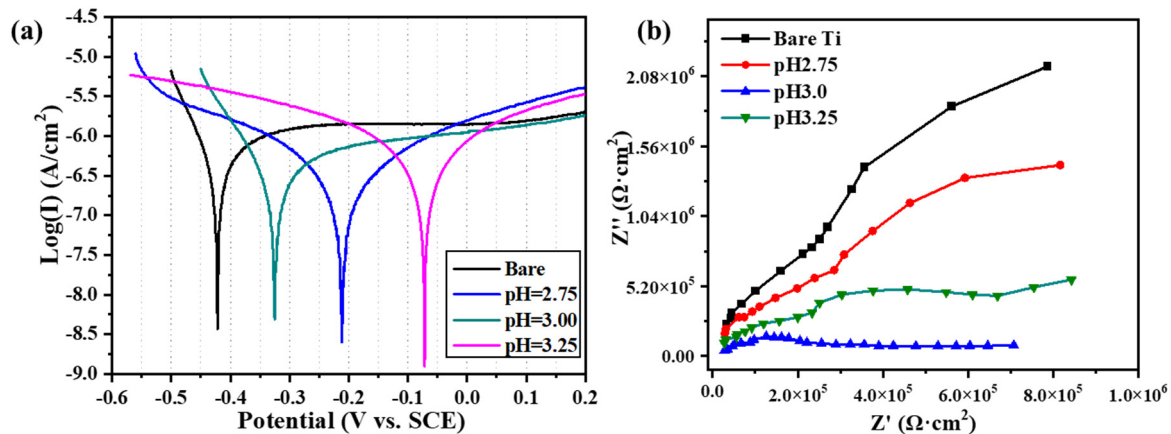


Figure 3. The electrochemical properties of bare and coated Ti samples fabricated with different pH values. (a) Potentiodynamic polarization, (b) Nyquist plots.

3.4. Cytocompatibility

Figure 4 shows the morphologies and cells number of BMSCs adhering to the surface of Ti substrates after being cultured for 3 days. Due to the incomplete structure of the coatings on Ti obtained at pH is 2.50 and 2.75, only two samples with pH 3.00 and 3.25 are selected for biological tests in this part. The results illustrate that BMSCs spread well and present elongated pseudopodia on the two kinds of coated Ti implants, while that cells demonstrate approximately spherical shape on the bare Ti samples (Figure 4 (A-C)). Additionally, the cck8 result proves that the adhered cells on the coated Ti surfaces are higher comparing with that on the Bare Ti. And the cells on the Sr-P coatings with pH=3.00 have the most beneficial for differentiation of BMSCs, as shown in Figure 4 (D). These data demonstrate that both the phase composition and microstructure of the conversion coating on Ti can affect the adhesion and differentiation of cells. In addition to the fine crystals structure of the coating, its mixture phases of SrHPO_4 and $\text{Sr}_3(\text{PO}_4)_2$ phases (as shown in Figure 1) can also promote cells differentiation.

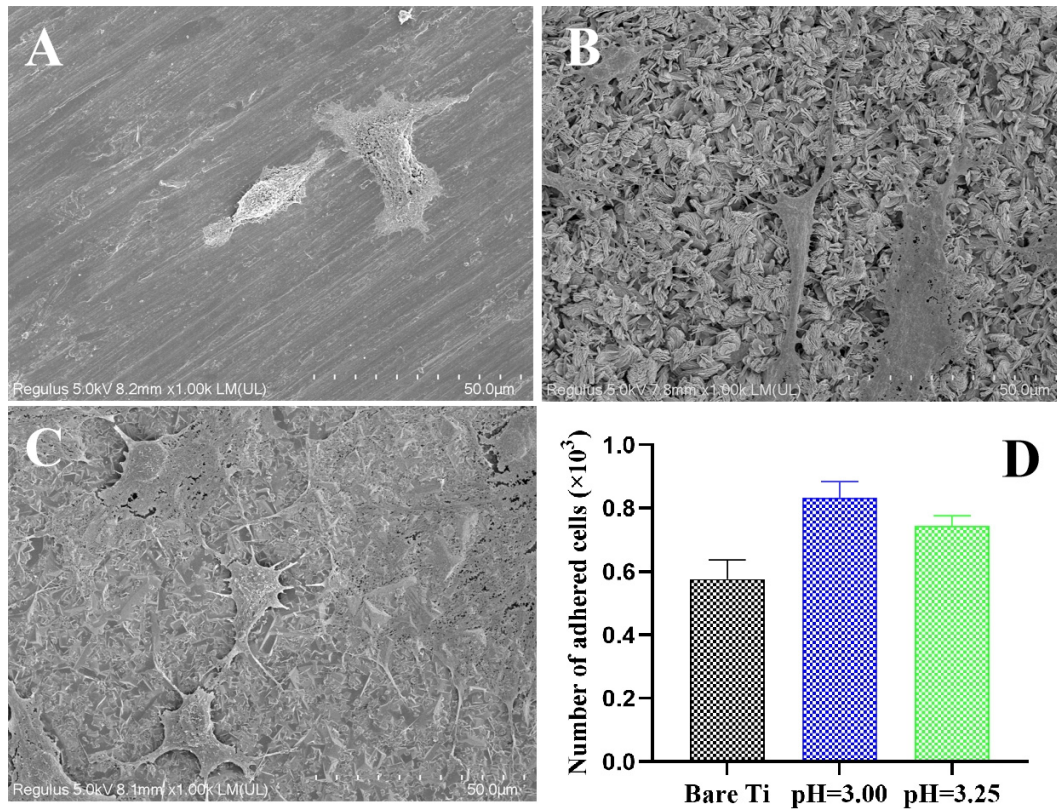
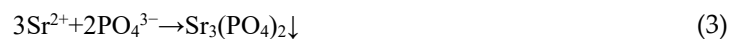
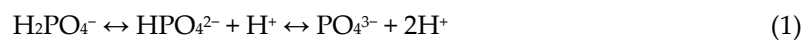


Figure 4. Morphologies and adhering number of BMSCs on bare and coated Ti samples with different pH values after cultured for 48 h. (A) Bare Ti, (B) pH=3.00, (C) pH=3.25 and (D) The number of adhered cells.

4. Discussion

This present study aims to provide a simple, effective and anticorrosion Sr-P chemical conversion coating by PCC processing to improve the properties of Ti substrates. Electrochemical reactions will proceed during PCC treatment, which includes obtaining electrons around Ti surface and losing electrons at cathode [27]. In PCC processing, all phosphate in solution is mainly treated as H_2PO_4^- , as pH changing from 2.50 to 3.25. When the discharge of hydrogen ions occurs at a cathode, the regional pH value near the Ti substrate increasing, which will result in forming HPO_4^{2-} and PO_4^{3-} according to the reaction of equation(1) [28]. When pH around Ti substrate continues to rise, SrHPO_4 will firstly precipitate from PCC solution due to its lower solubility. The reaction of equation (2) will happen and $\text{Sr}_3(\text{PO}_4)_2$ formed with increasing of pH value.



As shown in Figure 2, the number of crystals increases and their size reduces with the augment of pH value, whether the morphology of crystals is mainly plate-like at pH 2.5 and 2.75, or chiefly fine flaky-like at pH 3.00, or small bulk-like at pH 3.25. This result illustrates that the morphology of depositions on Ti substrate is markedly concerned with the H^+ ions in chemical solution, which is consistent with the results of some literature. Gashti et al. have shown that morphology of SrHPO_4 obtained via 0.8 M Na_2HPO_4 and 1 M SrCl_2 is denser and more compact than that obtained via 0.5 M Na_2HPO_4 and 0.5 M SrCl_2 [29]. A reasonable explanation for these phenomena is that relatively stable and low saturated degree always achieve large-sized single crystals, owing to the fact that low saturated degree could not generate crystal nucleus spontaneously but could only make crystals

grow along original nucleus (or crystal) until the completed crystal is formed [30]. In other words, when solution pH is increased, it is easier for H_2PO_4^- to transform to HPO_4^{2-} , the ingredient of SrHPO_4 , which leads to the higher saturated degree of SrHPO_4 . Naturally, accompanied by the increase of crystallization sites is the smaller size. Therefore, the crystals at pH 2.50 are large plate-like, the crystals at pH 3.00 are cluster-like and the crystals at pH 3.25 are denser and smaller. Specifically, the reason why both cluster-like and large plate-like crystals are formed is that the formations of large plate-like crystals augment pH value of the solution which further accelerates the formation of H_2PO_4^- and saturated degree. In addition, those fine flaky crystals that originally clustered at pH 3.00 distribute evenly on the Ti surface. Since SrHPO_4 is triclinic crystal and $a \neq b \neq c$, $\alpha \neq \beta \neq \gamma$, SrHPO_4 crystals can grow along with any direction and the irregular phases observed in the figure is mainly composed of SrHPO_4 . Meanwhile, $\text{Sr}_3(\text{PO}_4)_2$ matches the characteristic of hexagonal crystal, making its crystals to grow into a more regular shape, and showing a regular structure in the Figure 2D [31].

I_{corr} and E_{corr} derived from the measurements of specimens are used to evaluate the protective property of the coatings. Bare Ti shows good anticorrosion property because of the chemically stable passive film on the surface of Ti, as shown in Figure 3. The higher E_{corr} and lower I_{corr} value in the electrochemical test mean the coating has better anticorrosion property [32]. The coated Ti substrates have better corrosion resistance with the increasing pH values, which because the Sr-P conversion coatings are formed during PCC processing. The sample with pH=2.50 has only the sporadic plate-like SrHPO_4 crystals, as a precursor of $\text{Sr}_3(\text{PO}_4)_2$ phase [33], is generated, as shown in Figure 1. When this sample is incubated in SBF solution, the passive film TiO_2 still plays the anticorrosion major role. But the SrHPO_4 crystals on Ti can influence the electrochemical data of Figure 3. As pH value increases, the relative stable $\text{Sr}_3(\text{PO}_4)_2$ crystals growing and subsequently forming a coating on Ti substrate, which results in the corrosion resistant property is improving. The further rules and reasons will be researched in the future study.

The biological response of the cells around the implant is the result of the combined effect of the phase composition and microstructure of conversion coatings. So, their optimization should be considered comprehensively when designing the surface modification. As shown in Figure 4, The conversion coatings with pH 3.00 and 3.25 have obvious micr/ nano microstructure, which can provide excellent physical conditions for adhesion and differentiation of BMSC cells. Hulshof's research proved that the fate of cells can be determined through designing the surface microstructure and specific physicochemical properties[34]. The flaky- and bulk-like crystals on the Sr-P coatings allow the cell pseudopods to extend and embed into the gaps between the crystals, thus promote the cell adhesion and differentiation. Apart from the microstructure, the phase composition of the coating also significantly affects the biological behavior of the BMSC cells [16]. Under the influence of the culture medium, the two Sr-P conversion coatings can release the functional element Sr, which can significantly improve the differentiation ability of BMSCs, as shown in Figure 4 (D). For the coatings with pH=3.00, there are more SrHPO_4 and more Sr^{2+} ions are released, which leads to the better cell differentiation.

5. Conclusion

The Sr-P conversion coatings are successfully prepared on Ti substrates using a PCC processing in this work. The phase composition, morphology, corrosion resistance and cytocompatibility of coated Ti are different because of various pH values. During the conversion process, SrHPO_4 phase is first formed on the Ti surface. As pH is 3.00, the $\text{Sr}_3(\text{PO}_4)_2$ phase begins to form on the substrate. And the Sr-P phases content all gradually increases with the increase of pH value. When pH is 2.50, only a few sporadic plate-like SrHPO_4 crystals are generated on the substrate. With increasing of pH values, relative stable $\text{Sr}_3(\text{PO}_4)_2$ crystals are growing and subsequently forming a continuous coating on Ti substrate. The morphologies of conversion deposition on Ti present the structure from plate-like to flaky-like, and then evenly bulk-like microcrystals, as pH value changed from 2.50 to 3.25. The corrosion resistance of coated Ti improves because of the increase of $\text{Sr}_3(\text{PO}_4)_2$ phase in the coatings. In addition, Sr-P coatings also have good cytocompatibility. And the coating with pH=3.00 has the better differentiation due to its microstructure and phase composition.

Acknowledgments: This work was supported by the Shandong Provincial Natural Science Foundation (ZR2021MC176), the Key Research and Development Program of Shandong Province (2021ZLGX01).

Reference

- Long, M.; Rack, H. J., Titanium alloys in total joint replacement - a materials science perspective. *Biomaterials* **1998**, 19, (18), 1621-1639.
- Yuan, Z.; He, Y.; Lin, C.; Liu, P.; Cai, K., Antibacterial surface design of biomedical titanium materials for orthopedic applications. *Journal of Materials Science & Technology* **2021**, 78, 51-67.
- Shi, J.; Li, Y.; Gu, Y.; Qiao, S.; Zhang, X.; Lai, H., Effect of titanium implants with strontium incorporation on bone apposition in animal models: A systematic review and meta-analysis. *Scientific Reports* **2017**, 7, (1).
- Xu, A. T.; Xie, Y. W.; Xu, J. G.; Li, J.; Wang, H.; He, F. M., Effects of strontium-incorporated micro/nano rough titanium surfaces on osseointegration via modulating polarization of macrophages. *Colloids Surf B Biointerfaces* **2021**, 207, 111992.
- Yu, D.; Guo, S.; Yu, M.; Liu, W.; Li, X.; Chen, D.; Li, B.; Guo, Z.; Han, Y., Immunomodulation and osseointegration activities of Na₂TiO₃ nanorods-arrayed coatings doped with different Sr content. *Bioact Mater* **2022**, 10, 323-334.
- Liu, B.; Zhang, X.; Xiao, G. Y.; Lu, Y. P., Phosphate chemical conversion coatings on metallic substrates for biomedical application: A review. *Materials Science & Engineering C-Materials for Biological Applications* **2015**, 47, 97-104.
- Rajabalizadeh, Z.; Seifzadeh, D., Strontium phosphate conversion coating as an economical and environmentally-friendly pretreatment for electroless plating on AM60B magnesium alloy. *Surface and Coatings Technology* **2016**, 304, 450-458.
- Zhao, D.-W.; Liu, C.; Zuo, K.-Q.; Su, P.; Li, L.-B.; Xiao, G.-Y.; Cheng, L., Strontium-zinc phosphate chemical conversion coating improves the osseointegration of titanium implants by regulating macrophage polarization. *Chemical Engineering Journal* **2021**, 408.
- Li, Y.-B.; Lu, Y.-P.; Du, C.-M.; Zuo, K.-Q.; Wang, Y.-Y.; Tang, K.-L.; Xiao, G.-Y., Effect of Reaction Temperature on the Microstructure and Properties of Magnesium Phosphate Chemical Conversion Coatings on Titanium. *Molecules* **2023**, 28, (11).
- Du, C.; Zuo, K.; Ma, Z.; Zhao, M.; Li, Y.; Tian, S.; Lu, Y.; Xiao, G., Effect of Substrates Performance on the Microstructure and Properties of Phosphate Chemical Conversion Coatings on Metal Surfaces. *Molecules* **2022**, 27, (19).
- Zhao, D. W.; Du, C. M.; Zuo, K. Q.; Zhao, Y. X.; Xu, X. Q.; Li, Y. B.; Tian, S.; Yang, H. R.; Lu, Y. P.; Cheng, L.; Xiao, G. Y., Calcium-Zinc Phosphate Chemical Conversion Coating Facilitates the Osteointegration of Biodegradable Zinc Alloy Implants by Orchestrating Macrophage Phenotype. *Advanced Healthcare Materials* **2023**, 12, (9).
- Shen, X.; Zhang, Y.; Ma, P.; Sutrisno, L.; Luo, Z.; Hu, Y.; Yu, Y.; Tao, B.; Li, C.; Cai, K., Fabrication of magnesium/zinc-metal organic framework on titanium implants to inhibit bacterial infection and promote bone regeneration. *Biomaterials* **2019**, 212, 1-16.
- Han, W.; Fan, S.; Bai, X.; Ding, C., Strontium ranelate, a promising disease modifying osteoarthritis drug. *Expert Opinion on Investigational Drugs* **2017**, 26, (3), 375-380.
- Wang, W.; Yeung, K. W. K., Bone grafts and biomaterials substitutes for bone defect repair: A review. *Bioact Mater* **2017**, 2, (4), 224-247.
- Cheng, D.; Liang, Q.; Li, Y.; Fan, J.; Wang, G.; Pan, H.; Ruan, C., Strontium incorporation improves the bone-forming ability of scaffolds derived from porcine bone. *Colloids and surfaces. B, Biointerfaces* **2017**, 162, 279-287.
- Zhong, Z.; Wu, X.; Wang, Y.; Li, M.; Li, Y.; Liu, X.; Zhang, X.; Lan, Z.; Wang, J.; Du, Y.; Zhang, S., Zn/Sr dual ions-collagen co-assembly hydroxyapatite enhances bone regeneration through procedural osteo-immunomodulation and osteogenesis. *Bioact Mater* **2022**, 10, 195-206.
- Lode, A.; Heiss, C.; Knapp, G.; Thomas, J.; Nies, B.; Gelinsky, M.; Schumacher, M., Strontium-modified premixed calcium phosphate cements for the therapy of osteoporotic bone defects. *Acta biomaterialia* **2018**, 65, 475-485.
- Kunutsor, S. K.; Beswick, A. D.; Peters, T. J.; Gooberman-Hill, R.; Whitehouse, M. R.; Blom, A. W.; Moore, A. J., Health Care Needs and Support for Patients Undergoing Treatment for Prosthetic Joint Infection following Hip or Knee Arthroplasty: A Systematic Review. *PLOS ONE* **2017**, 12, (1), e0169068.

19. Ji, H.; Huang, Z.; Xia, Z.; Molokeev, M. S.; Atuchin, V. V.; Fang, M.; Liu, Y., Discovery of New Solid Solution Phosphors via Cation Substitution-Dependent Phase Transition in $M_3(PO_4)_2:Eu^{2+}$ ($M = Ca/Sr/Ba$) Quasi-Binary Sets. *The Journal of Physical Chemistry C* **2015**, 119, (4), 2038-2045.
20. Liu, B.; Xiao, G.-y.; Chen, C.-z.; Lu, Y.-p.; Geng, X.-w., Hopeite and scholizite coatings formation on titanium via wet-chemical conversion with controlled temperature. *Surface and Coatings Technology* **2020**, 384, 125330.
21. Zhang, X.; Xiao, G.-y.; Jiang, C.-c.; Liu, B.; Li, N.-b.; Zhu, R.-f.; Lu, Y.-p., Influence of process parameters on microstructure and corrosion properties of hopeite coating on stainless steel. *Corrosion Science* **2015**, 94, 428-437.
22. Wang, L.-l.; Xu, W.-h.; Xiao, G.-y.; Jiang, C.-c.; Zheng, Y.-z.; Lu, Y.-p., Chemical conversion of zinc-zinc phosphate composite coating on TC4 by galvanic coupling. *New Journal of Chemistry* **2017**, 41, (23), 14403-14408.
23. Phuong, N. V.; Lee, K. H.; Chang, D.; Moon, S., Effects of Zn^{2+} concentration and pH on the zinc phosphate conversion coatings on AZ31 magnesium alloy. *Corrosion Science* **2013**, 74, 314-322.
24. Liu, B.; Xiao, G.-y.; Lu, Y.-p., Effect of pH on the Phase Composition and Corrosion Characteristics of Calcium Zinc Phosphate Conversion Coatings on Titanium. *Journal of The Electrochemical Society* **2016**, 163, (8), C477-C485.
25. Zuo, K.-q.; Gong, Z.-y.; Xiao, G.-y.; Huang, S.-y.; Du, C.-m.; Liu, B.; Zhang, D.-s.; Lu, Y.-p., Microstructural evolution of strontium-zinc-phosphate coating on titanium via changing Zn^{2+} concentration in phosphate solution for enhanced osteogenic activity. *Surface and Coatings Technology* **2022**, 433.
26. Wang, Y. H.; Wei, Q. L.; Huang, Y. M., Preparation and adsorption properties of the biomimetic gamma-alumina. *Materials Letters* **2015**, 157, 67-69.
27. Liu, B.; Xiao, G. Y.; Jiang, C. C.; Zheng, Y. Z.; Wang, L. L.; Lu, Y. P., Formation initiation and structural changes of phosphate conversion coating on titanium induced by galvanic coupling and Fe^{2+} ions. *Rsc Advances* **2016**, 6, (79), 75365-75375.
28. Akhtar, A. S.; Wong, K. C.; Mitchell, K. A. R., The effect of pH and role of Ni^{2+} in zinc phosphating of 2024-Al alloy. Part I: Macroscopic studies with XPS and SEM. *Applied Surface Science* **2006**, 253, (2), 493-501.
29. Gashti, M. P.; Stir, M.; Hulliger, J., Growth of strontium hydrogen phosphate/gelatin composites: a biomimetic approach. *New Journal of Chemistry* **2016**, 40, (6), 5495-5500.
30. Scheel, H. J.; Fukuda, T., *Crystal Growth Technology*. J. Wiley: 2003; p 225-249.
31. Zhi-Zhan, L. W.-J. S. E.-w. Z. Y.-q. Y. Z.-W. C., Nucleating Mechanism of Oxide Crystal and Its Particle Size. *JOURNAL OF INORGANIC MATERIALS* **2000**, 15(5), 777-786.
32. Liang, Y.; Li, H.; Xu, J.; Li, X.; Li, X.; Yan, Y.; Qi, M.; Hu, M., Strontium coating by electrochemical deposition improves implant osseointegration in osteopenic models. *Experimental and therapeutic medicine* **2015**, 9, (1), 172-176.
33. Ishida, A.; Hori, S.; Tani, T.; Ikeda-Fukazawa, T.; Aizawa, M., Hydrothermal synthesis of single-crystal α -tristrontium phosphate particles. *Journal of the European Ceramic Society* **2017**, 37, (1), 351-357.
34. Hulshof, F. F. B.; Papenburg, B.; Vasilevich, A.; Hulsman, M.; Zhao, Y.; Levers, M.; Fekete, N.; de Boer, M.; Yuan, H.; Singh, S.; Beijer, N.; Bray, M.-A.; Logan, D. J.; Reinders, M.; Carpenter, A. E.; van Blitterswijk, C.; Stamatialis, D.; de Boer, J., Mining for osteogenic surface topographies: In silico design to in vivo osseointegration. *Biomaterials* **2017**, 137, 49-60.

Disclaimer/Publisher's Note: The statements, opinions and data contained in all publications are solely those of the individual author(s) and contributor(s) and not of MDPI and/or the editor(s). MDPI and/or the editor(s) disclaim responsibility for any injury to people or property resulting from any ideas, methods, instructions or products referred to in the content.